pISSN 1598-298X / eISSN 2384-0749
J Vet Clin 35(2) : 53-56 (2018)
http://dx.doi.org/10.17555/jvc.2018.04.35.2.53

Journal of Veterinary Clinics
www.ksvc.or.kr

Imaging Features of Hepatic Adenoma in a Dog with Atypical Computed Tomographic Findings

Hansol Jin, Byunggyu Cheon, Gahyun Lee, Seungjo Park, Ju-Hwan Lee* and Jihye Choi[1]

College of Veterinary Medicine, Chonnam National University, 77, Youngbong-ro, Buk-gu, Gwangju 500-757, Korea
**Chonnam National University Veterinary Teaching Hospital, 77, Youngbong-ro, Buk-gu, Gwangju 500-757, Korea*

(Received: August 09, 2017 / Accepted: February 27, 2018)

Abstract : Computed tomography (CT) findings of hepatic adenoma in veterinary medicine are variable and unlike in human medicine, not defined clearly. A 12-year-old neutered male Shih Tzu presented after a seizure, with weight loss, salivation, and cachexia. An abdominal mass was identified on radiography, and ultrasonographic images showed a mixed echo pattern with marked vascularity. CT showed that the mass originated from caudate lobe, was heterogeneously hypoattenuated compared with the hepatic parenchyma, and had irregular margins. Contrast enhanced CT showed that the mass enhanced like the surrounding liver parenchyma. However, it contained unenhanced areas and enhanced vessels were observed in the arterial phase at the periphery of the mass. The margins of mass were more enhanced in the venous phase than the arterial phase and the hypoattenuating regions within the mass were not enhanced. Greater enhancing in the venous phase is seen with adenomas; however, the heterogeneous enhancement pattern, especially the marginal vascular enhancement and internal hypoattenuating regions, is seen with malignancy. Although this is a single case of hepatic adenoma, the atypical enhanced pattern of this case can provide useful information to predict the malignancy of primary liver tumor.

***Key words* :** computed tomography, dog, hepatic adenoma, tumor.

Introduction

Primary hepatic tumors are uncommon and the incidence of hepatic tumors in dogs is 0.6-1.5% of total tumors (12). Primary hepatic tumors can be classified according to the cellular origin as hepatocellular, mesenchymal, cholangiohepatic, and neuroendocrine (12). Hepatocellular tumors include hepatocellular adenoma, hepatocellular carcinoma, and hepatoblastoma. Hepatocellular carcinoma is most common in dogs, while adenoma is most commonly reported in cats. Hepatocellular adenoma is a benign tumor of epithelial origin often identified as an incidental finding without clinical signs.

Diagnostic imaging is useful to investigate tumor location, size, internal structure, and distribution, and to determine therapy based on tumor staging and the presence of metastases (17). Radiography can identify tumor displacement of organs, for example caudal deviation of the gastric axis. However if the tumor is small there may be no radiographic findings (4,16,17). Ultrasonography can assess the tumor characteristics, internal structure, location, size, and anatomic relationship to adjacent organs, including the caudal vena cava and gall bladder (1,7,15,18,23). Hepatic tumors have various ultrasonographic signs regardless of histologic type, although hepatocellular carcinoma is usually hyperechoic (6,11,24).

Computed tomography (CT) is useful for staging tumors by assessing metastases to lymph nodes or other organs, detecting tumor size, and determining the tumor location, particularly when the tumor is too large to be localized by ultrasonography (8). Moreover, three-dimensional reconstruction of CT images defines the anatomic relationship between the tumor and adjacent blood vessels and organs. In human medicine, contrast enhanced CT study predicts the malignancy of hepatic tumor by evaluation of the enhancement pattern and vascular distribution of the mass (9,17). Hepatocellular carcinoma tends to be large and contain unenhanced areas within the tumor parenchyma. On contrast enhanced CT images, hepatocellular carcinoma shows marked enhancing from the central or marginal region with vessels feeding the tumor in the arterial phase. The images are hypoattenuated in the venous phase. In pre-contrast CT images, the density of hepatocellular adenomas is similar to normal hepatic parenchyma. Hepatocellular adenomas display a uniform enhancement pattern in the arterial phase. Uniform enhancement of the mass can also be observed in other benign lesions, including nodular hyperplasia; however, this pattern has never been reported in hepatic malignancy. Thus, uniform enhancement in the arterial phase is considered a characteristic contrast pattern of a benign hepatic tumor. Due to retention of the contrast agent in the tumor in the venous and delayed phase, hepatocellular adenomas show density similar to or higher than that of normal hepatic parenchyma (9).

Although contrast CT study is widely used to assess hepatic tumors and typical findings have been described in humans, CT has been used to assess hepatic tumors in a few dogs. The typical enhancement pattern of hepatic tumors in dogs has not been characterized. Therefore, there is need to inves-

[1]Corresponding author.
E-mail : imsono@jnu.ac.kr

tigate contrast CT patterns of hepatic tumors in a population of dogs (9,10). This report describes atypical CT features of a large hepatocellular adenoma in a dog.

Case

A 12-year-old, neutered male, Shih Tzu presented with a history of one seizure 1 hour prior to admission. This was the first seizure. Due to a 1-month history of weight loss, the dog had been prescribed medications for hepatic and pancreatic diseases from local clinic. On physical examination, the dog was cachexic and depressed. An abdominal mass was palpated in the cranial abdomen.

Complete blood count revealed normal hematocrit (52.7%; reference range, 37.3-61.7%), leukocytosis (19.95 K/uL; reference range, 5.05-16.76 K/uL), and neutrophilia (16.27 K/uL; reference range, 2.95-1.64 K/uL). Serum biochemistry revealed elevated levels of alkaline phosphatase (> 2,000 U/L; reference range, 23-212 U/L), alanine transaminase (> 1,000 U/L; reference range, 10-100 U/L), amylase (1748 U/L; reference range, 500-1500 U/L), and glucose (171 mg/dL; reference range, 70-143 mg/dL).

On abdominal radiography, a soft tissue density mass (10.2 × 9.4 cm in size) was identified caudal to the stomach in the right upper abdomen (Fig 1). On the lateral view, the mass displaced the stomach cranially and the small intestine caudally. On the ventrodorsal view the mass displaced the gastric body to the left and intestine caudally. The cardiac silhouette was slightly decreased. Based on the mass location and displacement of adjacent organs, the mass was suspected to originate from the liver, spleen, pancreas, or lymph node. Ultrasound images showed that the mass had a mixed echo pattern, with hyper- and hypo-echoic areas and color signal on conventional color Doppler examination (Fig 2). The mass appeared to originate from the right lateral or caudate liver lobe. The mass had an irregular contour with distinct mar-

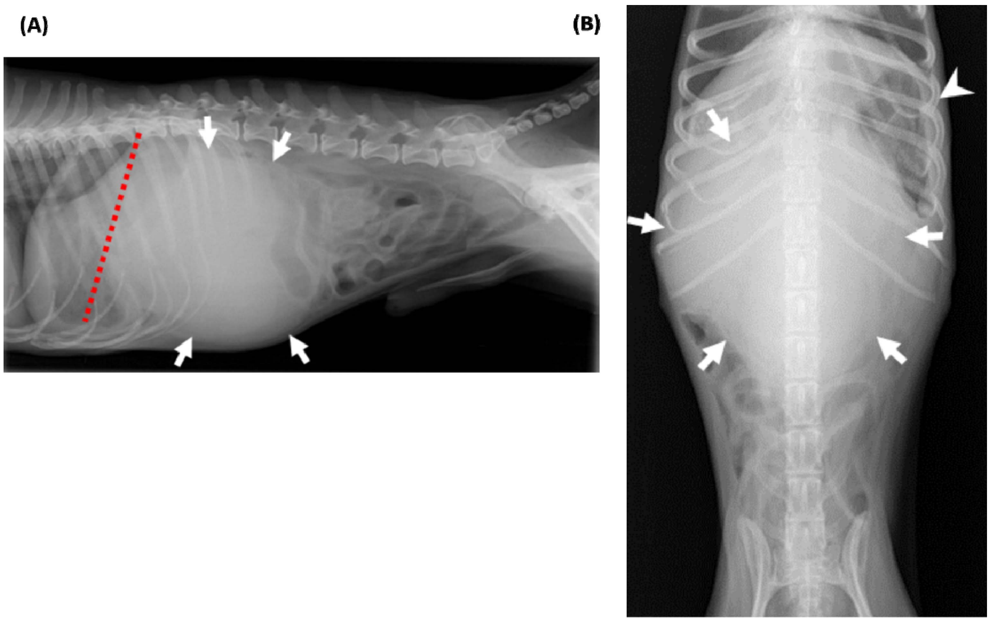

Fig 1. Abdominal radiographs of the mass. A soft tissue density mass (10.2 × 9.4 cm; arrows) is located in middle abdomen. In the lateral view (A) the mass displaces the gastric axis (dotted line) cranially and the small intestine caudally. In the ventrodorsal view (B) the mass displaces the stomach body (arrow heads) to left abdominal wall.

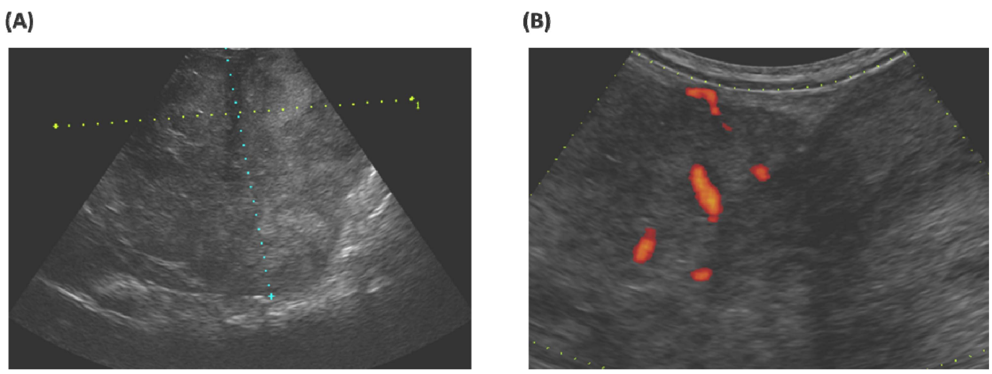

Fig 2. Abdominal ultrasonography of the mass. Note a heterogeneous mass (10 × 9 cm) with an irregular border (A). On the color Doppler examination (B), the mass shows blood flow signal.

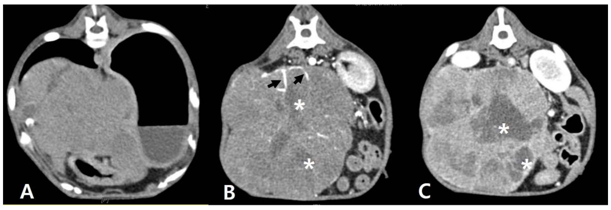

Fig 3. Computed tomographic images of the liver mass. On pre-contrast CT image (A), the mass is iso-attenuating with the adjacent liver parenchyma but containing hypoattenuating regions. After contrast agent injection, the unenhanced areas of the mass are heterogeneously enhanced (*). In the arterial phase, enhanced vessels (arrows) are seen from the periphery of the mass to the center (B). The mass in venous phase (C) shows increased enhancement when compared to the arterial phase, however, unenhanced areas (*) are still observed. Left side of the transverse CT image is right side of the patient.

gins without evidence of invasion into the adjacent organs. The remaining liver parenchyma appeared normal. There was no evidence of mesenteric edema, ascites, or reactive lymph node. Based on the ultrasonographic findings, the differential diagnosis for the mass included hepatocellular carcinoma, adenoma, and hemangiosarcoma.

CT examination was performed to determine if the mass could be surgically resected and to identify metastatic disease. Anesthesia was induced with an intramuscular injection of propofol (5.5 mg/kg; PropoFlo, Zoetics, MI) and maintained with isoflurane (Isoflurane, Rhodia Organique Fine LTD., UK). The density of the mass was similar to the normal liver; however, it contained multifocal hypoattenuating regions. The mass was large ($9.6 \times 9.2 \times 7.6$ cm) and occupied the upper abdomen (Fig 3). Contrast study was performed after intravenous injection of 880 mgI/kg iohexol (Omnihexol 300; Korea United Pharm Co, Korea). Arterial CT image were acquired at 9 sec and venous images at 28 sec. The mass enhanced similar to the adjacent liver parenchyma; however, unenhanced regions were identified within the mass, and enhanced vessels were observed in arterial phase from the marginal region. The mass was more enhanced in venous phase. On three-dimensional reconstruction, the mass originated from caudate lobe. Intestinal loops, the pancreas, and adjacent vascular structures were displaced. Based on CT study, primary hepatic tumor including adenoma and hepatocellular carcinoma was suspected. In particular, hepatic malignancy could not be ruled out because of vascular marking at the tumor margin.

There was no evidence of invasion or metastases, and surgical resection was recommended. However, due to the possibility of hepatic malignancy and the presence of seizure activity, the owner's requested euthanasia and necropsy. On gross examination, a dark reddish mass originating from the caudate liver lobe was adhered to the right side of the pancreas and the mesentery. Well-differentiated hepatocytes surrounded by fibro-connective tissue were observed and normal lobular structure was not evident within the mass on histologic examination. The mass was confirmed as hepatocellular adenoma.

Discussion

Hepatocellular adenoma has a favorable prognosis when not accompanied by necrosis; thus, adenoma should be differentiated from malignant carcinoma. In dogs, imaging features of hepatocellular adenoma have rarely been reported (5,6,9). This study described the imaging features of a large hepatocellular adenoma in a dog including radiography, ultrasonography, and CT. In the present case, the mass was identified caudal to the stomach in the right upper abdomen on radiography. The gastric axis was displaced cranially on lateral view, and gastric body to left and intestinal loops to caudal direction on ventrodorsal view. These organ displacements are compatible with a mass originating from the middle division of liver, right pancreas, or splenic body and tail.

Conventional ultrasonography is unable to distinguish the malignancy of a liver mass. In humans, blood flow has been used to distinguish benign and malignant hepatic tumors. Continuous flow can be seen in both tumors, and pulsatile flow is only observed in hepatocellular carcinoma (3,13,19,22). Power Doppler can evaluate tumor blood flow with greater sensitivity (2,4,20,21). In this case, the presence of blood flow within the tumor was assessed using color Doppler examination; however, the blood flow pattern could not exactly evaluated using spectral Doppler because the vessels were too small and tortuous.

Contrast CT study is useful to distinguish between hepatocellular adenoma and carcinoma (9). In triphasic CT studies, a uniform enhancement pattern in the arterial phase and highly maintained enhancement, compared with adjacent hepatic parenchyma, in the venous and delayed phases are characteristic features of the adenoma (9). This uniform enhancement of the adenoma on venous and delayed phase is considered due to blood retention within the mass. In the venous and delayed phases, hepatocellular carcinoma is enhanced to a lower degree when compared with normal liver. In this case, the mass enhanced similar to normal liver. However, the mass contained unenhanced regions, and there was vascular enhancement at the tumor margin, like a feeding vessel encountered in hepatocellular carcinoma. Tumor enhancement was greater in the venous phase when compared to the arterial phase; however, the mixed pattern of low-density or unenhanced areas could not define this case as an adenoma.

Primary liver tumors are classified as massive, nodular, and diffuse according to the extent and distribution of the lesions (14,16,20,21). This case was identified as a massive form because the mass had distinct margins.

Conclusion

In this case, a large hepatocellular adenoma described imaging features on radiography, ultrasonography, and CT findings. When compared with other hepatic tumor, this adenoma had atypical CT features including marginal vessels in the arterial phase and a heterogeneous enhancement pattern in the venous phase. The triphasic contrast CT pattern should be investigated to determine the accuracy of contrast CT study to differentiate between benign and hepatic malignancy in more large population of dogs. Although one case of hepatocellular adenoma is reported here, this study has clinical significance because it describes the atypical features of hepatocellular adenoma.

Acknowledgement

This study was supported by the Basic Science Research Program, through the National Research Foundation of Korea (NRF), funded by the Ministry of Science, ICT, and Future Planning (NRF-2018R1A2B6006775).

Reference

1. Barr F. Percutaneous biopsy of abdominal organs under ultrasound guidance. J Small Anim Pract 1995; 36: 105-113.
2. Bartolozzi C, Lencioni R, Paolicchi A, Moretti M, Armillotta N, Pinto F. Differentiation of hepatocellular adenoma and focal nodular hyperplasia of the liver: comparison of power Doppler imaging and conventional color Doppler sonography. Eur Radiol 1997; 7: 1410-1415.
3. Bates SM, Keller MS, Ramos IM, Carter D, Taylor K. Hepatoblastoma: detection of tumor vascularity with duplex Doppler US. Radiology 1990; 176: 505-507.
4. Evans SM. The radiographic appearance of primary liver neoplasia in dogs. Vet Radiol Ultrasound 1987; 28: 192-196.
5. Eves NG. Hepatocellular adenoma in a 12-year-old crossbred German shepherd dog. Can Vet J 2004; 45: 326-328.
6. Faverzani S, Chinosi S, Valenti P, Caniatti M. Comparison between ultrasonography and cytology of liver focal lesions and parenchyma in the dog and cat. Vet Res Commun 2006; 30: 293-296.
7. Feeney D, Johnston G, Hardy R. Two-dimensional, gray-scale ultrasonography for assessment of hepatic and splenic neoplasia in the dog and cat. J Am Vet Med Assoc 1984; 184: 68-81.
8. Fong Y, Kemeny N, Lawrence T. Cancer of the liver and biliary tree. In: De Vita VT, Hellman S, Rosenberg S, eds. Cancer: principles and practice of oncology. Philadelphia, USA: Lippincott Williams and Wilkins, 2001: 1178-1203.
9. Fukushima K, Kanemoto H, Ohno K, Takahashi M, Nakashima K, Fujino Y, et al. CT characteristics of primary hepatic mass lesions in dogs. Vet Radiol Ultrasound 2012; 53: 252-257.
10. Grazioli L, Federle MP, Brancatelli G, Ichikawa T, Olivetti L, Blachar A. Hepatic adenomas: Imaging and pathologic findings 1. Radiographics 2001; 21: 877-892.
11. Guillot M, D'Anjou MA, Alexander K, BEDard C, Desnoyers M, Beauregard G, et al. Can sonographic findings predict the results of liver aspirates in dogs with suspected liver disease? Vet Radiol Ultrasound 2009; 50: 513-518.
12. Hammer AS, Sikkema DA. Hepatic neoplasia in the dog and cat. Vet Clin North Am Small Anim Pract 1995; 25: 419-435.
13. Koito K, Namieno T, Morita K. Differential diagnosis of small hepatocellular carcinoma and adenomatous hyperplasia with power Doppler sonography. Am J Roentgenol 1998; 170: 157-161.
14. Lawrence HJ, Erb HN, Harvey H. Nonlymphomatous hepatobiliary masses in cats: 41 cases (1972 to 1991). Vet Surg 1994; 22: 365-368.
15. Léveillé R, Partington BP, Biller D, Miyabayashi T. Complications after ultrasound-guided biopsy of abdominal structures in dogs and cats: 246 cases (1984-1991). J Am Vet Med Assoc 1993; 203: 413-415.
16. Liptak JM, Dernell WS, Monnet E, Powers BE, Bachand AM, Kenney JG, et al. Massive hepatocellular carcinoma in dogs: 48 cases (1992-2002). J Am Vet Med Assoc 2004; 225: 1225-1230.
17. Liptak JM, MVetClinStud F, Dernell WS, Withrow SJ. Liver tumors in cats and dogs. Compend Contin Educ Pract Vet 2004; 36: 50-56.
18. Newell S, Selcer B, Girard E, Roberts G, Thompson JP, Harrison J. Correlations between ultrasonographic findings and specific hepatic diseases in cats: 72 cases (1985-1997). J Am Vet Med Assoc 1998; 213: 94-98.
19. Orr NM, Taylor KJ. Doppler detection of tumor vascularity. Clin Diagn Ultrasound 1990; 26: 149-163.
20. Patnaik A, Hurvitz A, Lieberman P, Johnson G. Canine hepatocellular carcinoma. Vet. Pathol 1981; 18: 427-438.
21. Post G, Patnaik A. Nonhematopoietic hepatic neoplasms in cats: 21 cases (1983-1988). J Am Vet Med Assoc 1992; 201: 1080-1082.
22. Taylor K, Ramos I, Carter D, Morse S, Snower D, Fortune K. Correlation of Doppler US tumor signals with neovascular morphologic features. Radiology 1988; 166: 57-62.
23. Vörös K, Vrabély T, Papp L, Horvath L, Karsai F. Correlation of ultrasonographic and patho morphological findings in canine hepatic diseases. J Small Anim Pract 1991; 32: 627-634.
24. Whiteley M, Feeney D, Whiteley L, Hardy R. Ultrasonographic appearance of primary and metastatic canine hepatic tumors. A review of 48 cases. J Ultrasound Med 1989; 8: 621-630.